Multi-scale Stochastic Dynamic Response Analysis of Offshore Risers with Lognormal Uncertainties

*Pinghe Ni [1], Yong Xia [2], Jun Li [3, 4, *], Hong Hao [3], Kaiming Bi [3], Haoran Zuo [3]*

[1] Key Laboratory of Urban Security and Disaster Engineering of Ministry of Education, Beijing University of Technology, Beijing, China

[2] Department of Civil and Environmental Engineering, The Hong Kong Polytechnic University, Hung Hom, Kowloon, Hong Kong

[3] Centre for Infrastructural Monitoring and Protection, School of Civil and Mechanical Engineering, Curtin University, Kent Street, Bentley, WA 6102, Australia

[4] State Key Laboratory of Coastal and Offshore Engineering, Dalian University of Technology, Dalian, China

Abstract: This paper presents a multi-scale stochastic dynamic analysis method for offshore structures. The uncertainties in the structural material parameters, such as mass density and Young's modulus, are considered. They are assumed to be lognormal distributions and represented by using the Karhunen–Loeve (KL) and Polynomial Chaos (PC) expansions. Since the variance of the output responses is unknown, the output vibration response is represented by using PC expansion. The multi-scale stochastic analysis is conducted with PC expansions of different orders representing responses at different DOFs defined as three categories, namely, important, less important and the least important ones. Iterated Order Reduced (IOR) model reduction technique is employed to remove the PC coefficients of slave DOFs. Two numerical examples are taken to verify the accuracy and efficiency of the proposed method for the multi-scale stochastic dynamic response analysis of offshore risers. The response statistics such as mean value and variance can be obtained from the proposed method.

The results are compared with those from Monte Carlo Simulation (MCS) and Stochastic Finite Element Method (SFEM). Results demonstrate that the computational demand for uncertainty evaluation is greatly reduced, and the accuracy of the results is maintained.

*Corresponding Author, Centre for Infrastructural Monitoring and Protection, School of Civil and Mechanical Engineering, Curtin University, Kent Street, Bentley, WA 6102, Australia. Email: junli@curtin.edu.au; LI.Jun@connect.polyu.hk, Tel.: +61 8 9266 5140; Fax: +61 8 9266 2681.

1 Introduction

Performance-based structural analysis and design are becoming a significant topic in civil engineering community. Structural performance assessment can more realistically be done in a probabilistic sense, since uncertainties inevitably exist in the dimensions, geometry, material properties, loading and the numerical modelling assumptions of structures (Haukaas and Der Kiureghian, 2004). Probabilistic structural analysis is receiving more attention in the last decades (Stefanou, 2009). Many approaches been proposed to simulate the random properties due to the uncertainties, i.e. Karhunen–Loeve (KL) expansion method (Huang et al., 2001), orthogonal series expansions (Stefanou, 2009) and optimal linear estimation method (Li and Der Kiureghian, 1993). With the realized random input, Monte Carlo Simulation (MCS) is a traditional method to evaluate the probabilistic characterization of the model output. Other methods, i.e. Neumann series expansion (Yamazaki et al., 1988), Polynomial Chaos (PC) expansion (Xiu and Karniadakis, 2002) and the first-order second-moment method (Dolinski, 1982) have also been developed to determine the stochastic characteristics of output with random input variables. Stochastic structural analysis has been widely performed in many engineering areas, e.g. settlement analysis of a foundation (Sudret and Der Kiureghian, 2000), reliability assessment of structures (Haldar and Mahadevan, 2000), and performance-based earthquake engineering (Kiureghian and Fujimura, 2009), etc.

With the growing needs for the exploitation of oil and gas in the deeper water, marine risers are pipe used in floating operations to convey drilling fluid and to guide tools between the drilling vessel and the wellhead at the ocean floor. Monitoring the conditions of marine risers is essential for the offshore industry since the failure of the risers may cause significant lost and catastrophic consequence.

With an increase in drilling operations in harsh environments, the requirements and limits of marine risers have become more essential due to uncertainties involved in response prediction and prolonged drilling programs. Many research works have been done to investigate the dynamic behavior of marine risers, i.e. vortex induced vibrations (Chen et al., 2015; Feng et al., 2017; Tsukada and Morooka, 2016; Wu et al., 2016). A detail review on the modelling and analysis techniques of flexible risers can be found in (Patel and Seyed, 1995). However, most of existing studies are based on deterministic analyses, which assumed that the system parameters were specific constant values.

Uncertainty analysis of marine structures gains a significant amount of attention in recent years. Alibrandi and Koh (2017) presented a study on stochastic dynamic analysis of a floating production system with the first order reliability method and Secant Hyperplane Method. The vessel model and marine riser were simplified as a 2-DOF model. The uncertainties of the output responses under random sea wave loading was evaluated. He and Low (2013) proposed a technique to predict the collision probability of risers. The random inputs, such as the drag coefficient, current, vessel motions and riser mass were considered. Yang and Wang (2013) utilized the surrogate model to evaluate the influences of random variables on the stability of pipeline. The uncertainties in the soil properties, structural modelling, and hydrodynamic loads were considered. Cabrera-Miranda and Paik (2017) evaluated the probabilistic distribution of loads. A metamodel was developed to predict the loads, such as axial tension waves, winds, and currents. Ni et al. (2018) performed the stochastic dynamic response analysis of marine risers considering Gaussian system uncertainties. Model reduction was employed to reduce the dimension of the stochastic dynamical system and therefore the computational demand in the stochastic dynamic response analysis.

Using Gaussian random fields to simulate the uncertain system parameters has been widely studied in the above literatures. However, the assumption is not necessarily true and suitable to model all the material properties, i.e. Young's modulus and yielding strength, etc. In the soil-structure system analysis, the material constitutive parameters were assumed to follow the lognormal distribution (Barbato et al., 2010). To study the uncertainty effect on the natural frequencies of a bridge, the Young's modulus of the bridge is considered having a lognormal distribution (Wan et al., 2017). Other research works on lognormal random inputs can be referred to (Barbato et al., 2013; Gupta and Arun, 2018; Saydam and Frangopol, 2013). Realizations of a Gaussian random field with a large coefficient of variation may include negative outcomes, which are physically meaningless. From a practical point of view, the lognormal random fields appear attractive in this sense because they are naturally positive valued (Sudret and Der Kiureghian, 2000).

The stochastic Young's modulus and mass density are assumed having lognormal distributions, represented with KL and PC expansions. The statistics of parameters are defined based on the design information and literatures. The stochastic output response is represented by using PC expansion. The accuracy of uncertainty analysis depends on the order of PC expansion. In this study, the degrees-of-freedom (DOFs) of the structure are classified into three categories, namely, important DOFs which will be represented with high order PC expansions, less important DOFs with low order PC expansions and unimportant DOFs being eliminated. High order PC expansions will be used for DOFs with high significance and interest. Iterated Order Reduced (IOR) method (Xia and Lin, 2004b) is employed to reduce the dimension of the stochastic system and reduce the computational demand. Those PC expansion coefficients associated with unimportant DOFs are to be removed, and the computational

efficiency is improved. Numerical studies on a simplified riser model with beam elements and a cylinder riser model with shell elements are conducted. The statistics of the responses of riser models obtained with the proposed approach are compared with those calculated from MCS and Stochastic Finite Element Method (SFEM). Results demonstrate that the accuracy and efficiency of the proposed approach are good by keeping the PC expansion coefficients associated with the main DOFs, based on the used IOR model reduction technique.

2 Representation of lognormal random inputs

2.1 PC expansion

PC expansion is an efficiency tool to model the stochastic processes. The first research work on PC expansion was developed by Wiener (1938), who used Hermite polynomials and Gaussian random variables to represent the stochastic processes. Xiu and Karniadakis (2002) found that the optimal exponential convergence rate cannot be generated when the Hermite polynomial is used to represent the non-Gaussian processes. The theory of PC expansion is briefly reviewed in this section and is used to represent the random inputs and outputs later. A random process $\alpha(\theta)$ can be treated as a function of the random input variable θ, with the following equation

$$
\begin{aligned}
\alpha(\theta) = a_0\psi_0 &+ \sum_{j1=1}^{\infty} a_{j1}\psi_1\left(\xi_{j1}(\theta)\right) \\
&+ \sum_{j1=1}^{\infty}\sum_{j2=1}^{i_1} a_{j1,j2}\psi_2\left(\xi_{j1}(\theta),\xi_{j2}(\theta)\right) \\
&+ \sum_{j1=1}^{\infty}\sum_{j2=1}^{j1}\sum_{j3=1}^{j2} a_{j1,j2,j3}\psi_3\left(\xi_{j1}(\theta),\xi_{j2}(\theta),\xi_{j3}(\theta)\right)+...
\end{aligned}
\tag{1}
$$

where ψ_p $(p=0, 1, 2, \ldots)$ are the p-th terms in the PC expansion, and $a_{j1, j2, j3}$ are deterministic coefficients.

To reduce the computational demand, the expansion in Eq. (1) is truncated. Taking a two-dimensional case for example, the PC approximation can be expressed as

$$
\begin{aligned}
\alpha(\theta) = & a_0\psi_0 + a_1\psi_1(\xi_1) + a_2\psi_1(\xi_2) \\
& + a_{11}\psi_2(\xi_1,\xi_1) + a_{21}\psi_2(\xi_1,\xi_2) + a_{22}\psi_2(\xi_2,\xi_2) \\
& + a_{111}\psi_3(\xi_1,\xi_1,\xi_1) + a_{211}\psi_3(\xi_2,\xi_1,\xi_1) + a_{221}\psi_3(\xi_2,\xi_2,\xi_1) + a_{222}\psi_3(\xi_2,\xi_2,\xi_2) + \ldots
\end{aligned}
\tag{2}
$$

A new polynomial functions Ψ_k is defined to replace ψ_k with one-to-one correspondence. Eq. (2) can be expressed in a matrix form as

$$
\alpha(\theta) = \sum_{k=0}^{\infty} \hat{a}_k \Psi_k(\xi(\theta))
\tag{3}
$$

where $\hat{a}_k$ are the deterministic PC coefficients. The two-dimensional expansion as shown in Eq. (2), in this case, can be expressed as,

$$
\alpha(\theta) = \hat{a}_0\Psi_0 + \hat{a}_1\Psi_1 + \hat{a}_2\Psi_2 + \hat{a}_3\Psi_3 + \hat{a}_4\Psi_4 + \hat{a}_5\Psi_5 \cdots
\tag{4}
$$

The polynomials $\Psi_k(\xi(\theta))$ are orthogonal and they satisfy the following relation

$$
\langle \Psi_k\xi(\theta), \Psi_l\xi(\theta) \rangle = \Psi_k^2\xi(\theta)\delta_{kl}
\tag{5}
$$

where δ_{kl} is the Kronecker delta. The symbol $\langle \bullet \rangle$ is the inner product, and the value of Ψ_k^2 can be calculated theoretically (Ghanem and Spanos, 2003).

2.2 KL expansion of lognormal random fields

KL expansion is combined with PC expansion to represent the lognormal random field of uncertainties in the material parameters. $H(\chi,\theta)$ and $\bar{H}(\chi)$ represent a second-order random

process and its mathematical expectation, respectively. $C_{\mathrm{cov}}(\chi_1, \chi_2)$ is the covariance matirx of $H(\chi, \theta)$. The covariance matrix $C_{\mathrm{cov}}(\chi_1, \chi_2)$ is bounded, symmetric and positive definite, which can be decomposed with the eigenvalues λ_n and eigenvectors $\varphi_n(\chi)$ as

$$C_{\mathrm{cov}}(\chi_1, \chi_2) = \sum_{n=0}^{\infty} \lambda_n \varphi_n(\chi_1) \varphi_n(\chi_2) \tag{6}$$

The eigenvectors are orthogonal and satisfy following equation

$$\int_V \varphi_q(\chi) \varphi_n(\chi) d\chi = \delta_{qn} \tag{7}$$

where δ_{qn} is the Kronecker delta function. Therefore, the eigenpairs $(\lambda_n, \varphi_n(\chi))$ can be calculated from the homogeneous Fredholm integral equation as

$$\int_V C_{\mathrm{cov}}(\chi_1, \chi_2) \varphi_n(\chi_2) d\chi_2 = \lambda_n \varphi_n(\chi_1) \tag{8}$$

$H(\chi, \theta)$ can be expressed as

$$H(\chi, \theta) = \bar{H}(\chi) + \underbrace{\sum_{n=1}^{\infty} \sqrt{\lambda_n} \varphi_n(\chi) \xi_n(\theta)}_{H_\sigma(\chi, \theta)} \tag{9}$$

where $\bar{H}(\chi)$ is the mean value of $H(\chi, \theta)$ and $\xi_n(\theta)$ is a set of uncorrelated standard Gaussian variables. Moreover, an explicit expression for $\xi_n(\theta)$ can be obtained by multiplying $H_\sigma(\chi, \theta)$ with $\varphi_n(\chi)$ and integrating through the domain V as follows

$$\xi_n(\theta) = \frac{1}{\sqrt{\lambda_n}} \int_V H_\sigma(\chi, \theta) \varphi_n(\chi) d\chi \tag{10}$$

Using the first m-th term eigenvalues and eigenvectors, the random field $H(\chi, \theta)$ can be approximated as

$$\hat{H}(\chi, \theta) = \bar{H}(\chi) + \sum_{n=1}^{m} g_n(\chi) \xi_n(\theta) \tag{11}$$

where $g_n(\chi)$ is the deterministic function $\sqrt{\lambda_n}\varphi_n(\chi)$.

Gathering the random variables $\xi_1(\theta)$, $\xi_2(\theta),\cdots,\xi_n(\theta)$ into a $n\times 1$ vector ξ and $g_1(\chi)$, $g_2(\chi),\cdots,g_n(\chi)$ into a $n\times 1$ vector $g(\chi)$, the lognormal random field can be approximated with $\hat{H}(\chi,\theta)$ as (Sudret and Der Kiureghian, 2000)

$$l(\chi)=\exp\left[\hat{H}(\chi,\theta)\right]=\exp\left[\bar{H}(\chi)+g(\chi)^T\xi\right] \tag{12}$$

Using PC expansion, Eq. (12) can be expressed as

$$l(\chi)=\sum_{n=0}^{M}l_n(\chi)\Psi_n(\xi) \tag{13}$$

where M is the number of polynomial functions, which depends on the number of KL expansion terms and the order of PC expansion p

$$M+1=\frac{(m+p)!}{(m)!p!} \tag{14}$$

and

$$l_n(\chi)=\frac{E\left(\exp\left[\hat{H}(\chi,\theta)\right]\Psi_n\right)}{E\left(\Psi_n^2(\xi)\right)} \tag{15}$$

where $E(\bullet)$ denotes the expectation.

Since the first coefficient corresponds to $\Psi_0=1$, we have

$$l_0(\chi)=\exp\left[\bar{H}(\chi)+\frac{1}{2}\sum_{n=1}^{M}g_i(\chi)^2\right]=\exp\left[\bar{H}(\chi)+\frac{1}{2}\sigma_g^2(\chi)\right] \tag{16}$$

where $\sigma_g(\chi)$ is the standard deviation of $\hat{H}(\chi,\theta)$. The other ones can be expressed as

$$l_n(\chi)=l_0(\chi)\frac{E\left[\Psi_n(\xi+g(\chi))\right]}{E\left[\Psi_n^2(\xi)\right]} \tag{17}$$

The details of closed-form solution can be found in (Sudret and Der Kiureghian, 2000).

3 Stochastic system with lognormal uncertainties

3.1 Equation of motion of a marine riser

A marine riser is a long and flexible pipe, which connects the sea floor with the offshore platform. The dynamic response of the structure can be calculated by using the idealized beam model and the fourth order partial differential equations (Cabrera-Miranda and Paik, 2019; Hong and Shah, 2018; Teixeira and Morooka, 2017)

$$EI(z,t)\frac{\partial^4 x(z,t)}{\partial z^4} - T(z,t)\frac{\partial^2 x(z,t)}{\partial z^2} + m(z,t)\frac{\partial^2 x(z,t)}{\partial t^2} + c(z,t)\frac{\partial x(z,t)}{\partial t} + p(z,t) = f(z,t) \quad (18)$$

where $EI(z,t)$, $T(z,t)$, $m(z,t)$, c, $p(z,t)$, $f(z,t)$ and z are the bending stiffness, the tension force, the mass per unit, the drag coefficient, the nonlinear restoring force, the hydrodynamic force, and the distance to the sea level, respectively, as shown in Figure 1.

The majority of the risers have a telescoping joint at the top, which enables the riser to move freely in the vertical direction. Therefore, the tension force $T(z,t)$ is not considered. The nonlinear drag force $p(z,t)$ can be represented by the duffing model, or polynomial types of nonlinearities (Li et al., 2018; Torres et al., 2015). Since the objective of this paper is to investigate the effect of uncertainties in the stochastic material properties on the lateral vibration response of the riser under the lateral sea wave loads, the nonlinear drag force is also neglected. When the finite element method is applied to study the dynamic behavior of marine risers (Spanos and Chen, 1980), Eq. (18) can be written as

$$m\ddot{x}(t) + c\dot{x}(t) + kx(t) = f(t) \quad (19)$$

where k, c and m denote the stiffness, damping and mass matrices of the riser, respectively; $x(t)$, $\dot{x}(t)$ and $\ddot{x}(t)$ are the displacement, velocity and acceleration responses, respectively. $f(t)$ is the applied sea wave loading on the riser. The Rayleigh damping model is used in this study.

In this study, the lognormal uncertainties in the structural parameters are considered in the stochastic response analysis and a multi-scale stochastic analysis approach is proposed to improve the computational efficiency and keep the accuracy. This is the main innovation of this paper, which is extended based on a previous study (Ni et al., 2018). The stochastic wave loading is given by Morison equation (Koh et al., 2018; Zuo et al., 2017). It should be noted that validations of numerical model and sea wave loading are not within the scope of this paper. Verifications of simulation results are presented by comparing the results from the proposed multi-scale analysis method with those from MCS and SFEM.

3.2 Hydrodynamic force

The sea wave loading is modeled by the Joint North Sea Wave Observation Project (JONSWAP) spectrum (Walden et al., 1973) with Morison equation (Veritas, 2000). First, the sea surface elevation is stochastically generated

$$S_{\eta\eta} = \alpha g^2 (2\pi)^{-4} f^{-5} \exp\left[-\frac{5}{4}\left(\frac{f_m}{f}\right)^4\right] \gamma^{\exp\left[-\frac{(f-f_m)^2}{2\sigma^2 f_m^2}\right]} \tag{20}$$

where, η, γ and g are the the sea surface elevation, the peak enhancement factor, and gravitational acceleration, respectively. The peak enhancement factor γ is usually given as 3.3 and f is the wave frequency in Hz. The other parameters in Eq. (20) are obtained as

$$\alpha = 0.076\left(v_{10}^2\right)^{-0.22} \tag{21}$$

$$f_m = \frac{11}{\pi}\left(v_{10}F/g^2\right)^{-1/3} \tag{22}$$

$$\sigma = \begin{cases} 0.07, & f \le f_m \\ 0.09, & f > f_m \end{cases} \tag{23}$$

where F is the fetch length and v_{10} is the mean wind velocity at 10 m above the sea surface. After the

sea surface elevation spectrum $S_{\eta\eta}$ is obtained, the sea surface elevation can be simulated in the time

domain as

$$\eta(t) = \sum_{i=1}^{n} \sqrt{2\Delta_\omega S_{\eta\eta}(\omega_i)}\cos\left(\omega_i t + \varphi(\omega_i)\right) \tag{24}$$

where $\varphi(\omega_i)$ is the random phase angle uniformly distributed over the range of $0 \sim 2\pi$. The

transverse sea wave force per unit length of the riser can be estimated from Morison equation (Veritas,

2000) as

$$f(t) = \frac{1}{2}\rho_{water}C_d |v_x| v_x + \frac{\pi}{4}\rho_{water}C_m d_p^2 a_x \tag{25}$$

where C_d and C_m are the drag and inertia coefficients, respectively, ρ_{water} is the sea water density and

d_p is the outer diameter of the riser. The velocity v_x and acceleration a_x of water particles in the

horizontal direction can be found in (Zuo et al., 2017), which are not introduced in details for

conciseness.

It is interesting to investigate the riser systems with different boundary conditions, the effects of

floating vessel motions, geometric nonlinearity and more sophisticated riser models. These factors play

an important role in the uncertainty analysis. The details of a riser model without the presence of a

floating vessel are described, and this model is taken as an example for the stochastic dynamic response

analysis. It should be noted that the main objective of this paper is to develop a multi-scale stochastic

dynamic analysis method and evaluate the effect of uncertainties in system parameters with lognormal

distributions on the dynamic responses.

3.3 Representation of the system parameters

The combination of KL and PC expansions is used to define the uncertain system parameters with

lognormal distributions as discussed in Section 2.2. In this study, the material parameters such as mass

density and Young's modulus, are represented as lognormal random fields. The mass density $\rho(\chi,\theta)$

and Young's modulus $E(\chi,\theta)$ can be approximated as

$$\hat{\rho}(\chi,\theta) = \sum_{i1=0}^{M_\rho} \rho_{i1}(\chi)\Psi_{i1}(\xi) \tag{26}$$

$$\hat{E}(\chi,\theta) = \sum_{i2=0}^{M_E} E_{i2}(\chi)\Psi_{i2}(\xi) \tag{27}$$

Substituting Eq. (26) into Eq. (19), the mass matrix of the stochastic system is written as

$$M(\theta) = \sum_{i1=0}^{M_\rho} \tilde{M}_{i1}(\chi)\Psi_{i1}(\xi) \tag{28}$$

$$\tilde{M}_{i1} = \sum_{i=1}^{ne} \bar{M}_i^e = \sum_{i=1}^{ne} \left(\int N^T \left(\rho_{i1}(\chi) A \right) N dl \right) \tag{29}$$

where N and A are the shape function and cross-sectional area, respectively.

Similarly, the stiffness matrix can be calculcated with

$$K(\theta) = \sum_{i2=0}^{M_E} \tilde{K}_{i2}(\chi)\Psi_{i2}(\xi) \tag{30}$$

In this paper, the Rayleigh damping matrix is used. The damping matrix considering the

uncertainties is expressed as

$$C = \alpha M(\theta) + \beta K(\theta) = \alpha \left(\sum_{i1=0}^{M_\rho} \Psi_{i1}(\xi) M_{i1} \right) + \beta \left(\sum_{i2=0}^{M_E} \Psi_{i2}(\xi) K_{i2} \right) \tag{31}$$

3.4 Representation of responses

A random dimension vector θ is used to represent the spatial–temporal dimension. The response vectors of the stochastic system are expressed as (Xiu and Karniadakis, 2003)

$$\boldsymbol{x}(t,\theta) = \left[x_1(t,\theta), x_2(t,\theta), \cdots, x_{dof}(t,\theta) \right]^T \tag{32a}$$

$$\dot{\boldsymbol{x}}(t,\theta) = \left[\dot{x}_1(t,\theta), \dot{x}_2(t,\theta), \cdots, \dot{x}_{dof}(t,\theta) \right]^T \tag{32b}$$

$$\ddot{\boldsymbol{x}}(t,\theta) = \left[\ddot{x}_1(t,\theta), \ddot{x}_2(t,\theta), \cdots, \ddot{x}_{dof}(t,\theta) \right]^T \tag{32c}$$

where the subscript represents the DOF number of the structure.

Because the spatial correlation of nodal acceleration $\ddot{\boldsymbol{x}}(t,\theta)$, velocity $\dot{\boldsymbol{x}}(t,\theta)$ and displacement $\boldsymbol{x}(t,\theta)$ are unknown, the stochastic output responses can be represented by the PC expansions according to Eq. (3) with truncations (Xiu and Karniadakis, 2002)

$$\boldsymbol{x}(t,\theta) = \sum_{j=0}^{M_t} \Psi_j(\theta) \boldsymbol{U}^j(t) \tag{33a}$$

$$\dot{\boldsymbol{x}}(t,\theta) = \sum_{j=0}^{M_t} \Psi_j(\theta) \dot{\boldsymbol{U}}^j(t) \tag{33b}$$

$$\ddot{\boldsymbol{x}}(t,\theta) = \sum_{j=0}^{M_t} \Psi_j(\theta) \ddot{\boldsymbol{U}}^j(t) \tag{33c}$$

where $\boldsymbol{U}^j(t)$ is the vector of PC expansion coefficients of $\boldsymbol{x}(t,\theta)$; $\dot{\boldsymbol{U}}^j(t)$ and $\ddot{\boldsymbol{U}}^j(t)$ are the first and second derivatives of the coefficient vector $\boldsymbol{U}^j(t)$, respectively. M_t is the dimension of PC expansion, which can be calculated as (Sudret and Der Kiureghian, 2000)

$$M_t + 1 = \frac{(K_\rho + K_E + p_r)!}{(K_\rho + K_E)! p_r!} \tag{34}$$

14

where p_r is the order of the PC expansion of the output responses, K_ρ and K_E are the numbers of KL expansion terms for the mass density and Young's modulus, respectively.

Substituting Eqs. (28), (30) and (33) into Eq. (19) without considering the uncertainty in the damping matrix, we have

$$\left(\sum_{i1=0}^{M_\rho} \Psi_{i1}(\theta) M_{i1}\right)\left(\sum_{j=0}^{M_t} \Psi_j(\theta)\ddot{U}^j(t)\right) + C\left(\sum_{j=0}^{M_t} \Psi_j(\theta)\dot{U}^j(t)\right)$$
$$+ \left(\sum_{i2=0}^{M_E} \Psi_{i2}(\theta) K_{i2}\right)\left(\sum_{j=0}^{M_t} \Psi_j(\theta)U^j(t)\right) = F(t) \tag{35}$$

Taking the inner product on both sides of the equation with $\Psi_k(\theta)$ and employing the orthogonal property in Eq. (35), we have

$$\sum_{j=0}^{M_t}\sum_{i1=0}^{M_\rho}\left\langle \Psi_{i1}(\theta)\Psi_j(\theta), \Psi_k(\theta)\right\rangle M_{i1}\ddot{U}^j(t) + \sum_{j=0}^{M_t}\left\langle \Psi_j(\theta), \Psi_k(\theta)\right\rangle C\dot{U}^j(t)$$
$$+ \sum_{j=0}^{M_t}\sum_{i2=0}^{M_E}\left\langle \Psi_{i2}(\theta)\Psi_j(\theta), \Psi_k(\theta)\right\rangle K_{i2}U^j(t) = \left\langle F_f, \Psi_k(\theta)\right\rangle \tag{36}$$

Rewriting Eq. (36) in the matrix multiplication form, we have

$$\begin{bmatrix} M_s^{(0,0)} & M_s^{(0,1)} & \cdots & M_s^{(0,M_t)} \\ M_s^{(1,0)} & M_s^{(1,1)} & \cdots & M_s^{(1,M_t)} \\ \vdots & \vdots & \ddots & \vdots \\ M_s^{(M_t,0)} & M_s^{(M_t,1)} & \cdots & M_s^{(M_t,M_t)} \end{bmatrix}\begin{bmatrix} \ddot{U}^0(t) \\ \ddot{U}^1(t) \\ \vdots \\ \ddot{U}^{M_t}(t) \end{bmatrix} + \begin{bmatrix} C_s^{(0,0)} & C_s^{(0,1)} & \cdots & C_s^{(0,M_t)} \\ C_s^{(1,0)} & C_s^{(1,1)} & \cdots & C_s^{(1,M_t)} \\ \vdots & \vdots & \ddots & \vdots \\ C_s^{(M_t,0)} & C_s^{(M_t,1)} & \cdots & C_s^{(M_t,M_t)} \end{bmatrix}\begin{bmatrix} \dot{U}^0(t) \\ \dot{U}^1(t) \\ \vdots \\ \dot{U}^{M_t}(t) \end{bmatrix}$$
$$+ \begin{bmatrix} K_s^{(0,0)} & K_s^{(0,1)} & \cdots & K_s^{(0,M_t)} \\ K_s^{(1,0)} & K_s^{(1,1)} & \cdots & K_s^{(1,M_t)} \\ \vdots & \vdots & \ddots & \vdots \\ K_s^{(M_t,0)} & K_s^{(M_t,1)} & \cdots & K_s^{(M_t,M_t)} \end{bmatrix}\begin{bmatrix} U^0(t) \\ U^1(t) \\ \vdots \\ U^{M_t}(t) \end{bmatrix} = \begin{bmatrix} F^0(t) \\ F^1(t) \\ \vdots \\ F^{M_t}(t) \end{bmatrix} \tag{37}$$

where

$$K_s^{(j,k)} = \sum_{i2=0}^{M_E}\left\langle \Psi_{i2}(\theta)\Psi_j(\theta), \Psi_k(\theta)\right\rangle K_{i2} \qquad (j,k=0,1,2,\cdots,M_t) \tag{38a}$$

$$M_s^{(j,k)} = \sum_{i1=0}^{M_\rho}\left\langle \Psi_{i1}(\theta)\Psi_j(\theta), \Psi_k(\theta)\right\rangle M_{i1} \qquad (j,k=0,1,2,\cdots,M_t) \tag{38b}$$

15

$$C_s^{(j,k)} = \Psi_k^2(\theta)\delta_{jk}C \qquad\qquad (j,k=0,1,2,\cdots,M_t) \qquad\qquad (38c)$$

$$F^k = \langle f(t), \Psi_k(\theta)\rangle = \begin{cases} f(t), k{=}0 \\ 0, k{=}1,2,3,\cdots,M_t \end{cases} \qquad\qquad (38d)$$

Similarly, we have

$$C_s^{(j,k)} = \alpha\left(\sum_{i1}^{M_\rho}\langle\Psi_{i1}(\theta)\Psi_j(\theta),\Psi_k(\theta)\rangle M_{i1}\right) + \beta\left(\sum_{i2}^{M_E}\langle\Psi_{i2}(\theta)\Psi_j(\theta),\Psi_k(\theta)\rangle K_{i2}\right) \qquad (39)$$

Eq. (37) can then be simplified as

$$M_s\ddot{U}_s(t) + C_s\dot{U}_s(t) + K_sU_s(t) = F_s(t) \qquad\qquad (40)$$

With the above derived equation, the coefficients of PC expansion can be solved with mode superposition method (Borino and Muscolino, 1986).

3.5 Multi-scale Uncertainty Quantification with Model reduction

When only the first several terms of KL expansion and a low order of PC expansion are used to represent the random input and outputs, the matrix size in Eq. (39) will increase significantly. It takes a long time to obtain the PC coefficients. Model reduction technique gains many attentions in recent years and many methods, such as Guyan method (Guyan, 1965), Iterated Improved Reduced System (IIRS) technique (Friswell et al., 1995) and IOR method (Xia and Lin, 2004b) have been developed. Model reduction methods have been successfully used in the areas of structural condition assessment (Li and Law, 2012) and sensitivity analysis (Weng et al., 2017). It has been reported that IOR method has a faster convergence ratio and better model reduction results (Xia and Lin, 2004a). In this study, IOR is employed to reduce the dimension of the stochastic dynamic system and therefore the computational demand. Only the essential PC expansion coefficients are preserved in the calculation.

Multi-scale uncertainty quantification can be achieved with model reduction technique as shown in Figure 2. The nodes in a structure can be classified into three categories, i.e. i) very important ones. For these nodes, PC expansion with a high order will be used to represent the random output; ii) less important ones. A low order PC expansion will be used; and iii) the least important ones. The statistical responses of these least important nodes are not of interest, and the corresponding coefficients of PC expansion can be eliminated. These coefficients to be eliminated are defined as the slave DOFs, and the others with high and low orders are defined as the master DOFs.

To apply model reduction technique in the stochastic response analysis with Eq. (40), K_s and M_s can be rewritten in a partitioned form as

$$K_s = \begin{bmatrix} K_{mm} & K_{ms} \\ K_{sm} & K_{ss} \end{bmatrix}, \quad M_s = \begin{bmatrix} M_{mm} & M_{ms} \\ M_{sm} & M_{ss} \end{bmatrix} \tag{41}$$

where m and s denote the master and slave DOFs, respectively.

The computational steps can be summarized as follows

Step 1: Initialization with $t^{(0)} = t_G = -K_{ss}^{-1} K_{ms}^T$, $T_G = \begin{bmatrix} I, t_G \end{bmatrix}^T$, $K_G = T_G^T K T_G$ and $M_d^{(0)} = T_G^T M T_G$.

Step 2: Obtain the transformation matrix $T^{(k)} = \begin{bmatrix} I, t^k \end{bmatrix}^T$, where

$$t^{(k)} = t_G + K_{ss}^{-1} \left(M_{ms} + M_{ss} t^{(k-1)} \right) \left[M_d^{k-1} \right]^{-1} K_G \tag{42}$$

$$M_d^{(k-1)} = \left[M_{ss} + M_{ms} t^{(k-1)} \right] + t_G^T \left[M_{ms}^T + M_{ss} t^{(k-1)} \right] \tag{43}$$

Step 3: The reduced system matrices are obtained as

$$M_r^{(k)} = \left[T^{(k)} \right]^T M T^{(k)} \quad \text{and} \quad K_r^{(k)} = \left[T^{(k)} \right]^T K T^{(k)} \tag{44}$$

Step 4: Repeat Step 2 and Step 3 until the convergence criteria are satisfied. The convergence

criteria is defined as

$$\frac{\left\| \Lambda_{mm}^{(it)} - \Lambda_{mm}^{(it-1)} \right\|}{\left\| \Lambda_{mm}^{(it)} \right\|} \leq Tol \tag{45}$$

where $\Lambda_{mm}^{(it)}$ are the eigenvalues of the reduced system.

The Rayleigh damping is used for the stochastic system with a reduced dimension

$$\boldsymbol{C}_r = \alpha \boldsymbol{M}_r + \beta \boldsymbol{K}_r \tag{46}$$

The reduced stochastic system matrices, i.e. $\boldsymbol{M}_r$, $\boldsymbol{K}_r$ and $\boldsymbol{C}_r$, are used for the stochastic dynamic

response analysis. The PC expansion coefficients, namely $\ddot{\boldsymbol{U}}_r(t)$, $\dot{\boldsymbol{U}}_r(t)$ and $\boldsymbol{U}_r(t)$, of the reduced

system, are calculated by using the mode superposition method (Borino and Muscolino, 1986). After

the coefficients of PC expansion are obtained, the mean value of nodal displacements $MEAN_U$ can be

evaluated as

$$MEAN_U = \boldsymbol{U}_r^0(t) \tag{47}$$

The variance of nodal displacements VAR_U is obtained as

$$VAR_U = \sum_{j=1}^{P_l} \left[\boldsymbol{U}_r^j(t) \right]^2 \Psi_j^2(\theta) \quad \text{or} \quad \sum_{j=1}^{P_h} \left[\boldsymbol{U}_r^j(t) \right]^2 \Psi_j^2(\theta) \tag{48}$$

where P_l and P_h are the dimensions of low order and high order PC expansions, respectively.

4 Numerical Studies

4.1 Beam model

In this section, numerical simulations on an offshore riser simulated by using Euler beam elements

will be conducted. The details of the two-dimensional finite element model are shown in Figure 3. The

18

marine riser has a length of 100m and outer diameter of 0.1524m. The structure is simulated with 20 elements and each element has 2 node and 4 DOFs. Totally, there are 40 DOFs for the numerical model. The riser has a fixed end at the bottom and the free end at the top. The vertical deformation caused by the floating vessel motions in waves is not considered in this study due to the large size of the stochastic system matrices and intensive computational requirement. Only the uncertainties in the structural material properties will be considered. The mean values of flexural rigidity and the mass per unit length are 4×10^{10} Nm² and 15 kg/m, respectively, which are assumed as two independent lognormal random variables. In this example, the spatial correlation is expressed by an exponential covariance function as

$$C_{\mathrm{cov}}\left(z_1, z_2\right) = \sigma_g^2 e^{-\left(\left|z_1 - z_2\right|^2 / a^2\right)} \tag{49}$$

where σ_g is the standard deviation of the Gaussian random field. The parameter a is the correlation length and the expression $\left|z_1 - z_2\right|$ is the distance between two points of interest, respectively.

When the designed lognormal distribution has a mean value of μ_l and standard deviation of σ_l, the corresponding value for the Gaussian distribution (μ_g and σ_g) are

$$\left(\sigma_g\right)^2 = \ln\left[\left(\frac{\sigma_l}{\mu_l}\right)^2 + 1\right] \tag{50}$$

$$\mu_g = \ln\left(\mu_l\right) - \frac{1}{2}\left(\sigma_g\right)^2 \tag{51}$$

The correlation length is in this study 50m and 20% uncertainties in the flexural rigidity and mass density are considered. To simulate the lognormal random field, the first six terms of eigenvectors and eigenvalues as described in Eq. (11) are used, and the designed lognormal distribution can be represented with Eq. (13). Different orders of PC expansions is performed to evaluate accuracy of the

lognormal random field. The first, second, and third order of PC expansions are studied. The Probability Density Function (PDF) and Cumulative Distribution Function (CDF) are then obtained. Figure 4 shows the statistical distribution properties of the flexural rigidity, i.e. PDF and CDF, comparing with their analytical values. The results with different orders of PC expansions are shown and the comparison indicates that a higher order of PC expansion will obtain a better accuracy to represent the lognormal random input. In the following studies, the third order PC expansion is selected to simulate the lognormal distributions of uncertain system material properties, i.e. flexural rigidity and mass density.

The simulated marine riser is subjected to sea wave loading with zero initial condition. To simulate the sea wave loading with Eq. (25), the following parameters are used: ρ_{water}=1030 kg/m^3, C_d=1.36, C_m=2, v_{10}=15 m/s, F=20000, f_m=0.245 Hz, and d_p=0.1524m. Figure 5 shows the sea wave loading generated from the JONSWAP spectrum and Morison equation. The full current load is applied from z=100 to 70 m, and the load reduces linearly from z=70 to the ocean floor z=0.

The uncertainty in damping is also considered in this study. Rayleigh damping model is used and the coefficients are α=0.6263 and β=0.0003, respectively. These two coefficients are obtained from the first two natural frequencies without considering the uncertainties. In this study, the responses under the sea wave loads are analyzed. The vertical loading from the floating platform to the top end of the riser is not considered.

SSFEM and MCS method are carried out to verify the accuracy of the proposed approach. In the MCS method, 50,000 simulations are conducted to obtain the reference statistical properties. These calculations for uncertainty analysis take 16 hours by using a computer of an i7-3770 CPU and 24 GB

RAM. A convergence study is performed first to check the statistics with different numbers of simulations. Statistical results of the displacement response at the top in the horizontal direction are evaluated and shown in Figure 6. These results verify that the statistics from 50,000 simulation runs is accurate enough and they can be taken as baseline for comparison in the subsequent studies. The results from SFEM with second and third order PC expansion will be discussed later.

In multiscale stochastic dynamic analysis, the vibration responses are represented by using the third order PC expansion. The responses of the rotational DOFs are usually not important and of intereste in the response analysis. These DOFs are defined as no important, and their PC coefficients are defined as the slave DOFs. The horizontal translations from Nodes 1-10 are defined as less important DOFs, and low order PC expansions (the 2nd order) are used. The horizontal translations of Nodes 11-20 are defined as important ones, and high order PC expansions are used. This is shown in Figure 7. Since these DOFs of the top part of the riser usually have larger responses, they are therefore considered as the important ones. The nodes in the bottom part of the riser are assumed as less important ones. For the less important nodes, only the PC coefficients in the first and second order terms are selected as the master DOFs. All the three order terms of PC coefficients of the important nodes are defined as the master DOFs.

The calculated horizontal deformations at the top end of the riser from MCS, SFEM and the proposed approach are shown in Figure 8. The mean values of these methods are almost the same as shown in Figure 8(a), and the variances are also in a very good agreement as shown in Figure 8(b). The horizontal deformation at the middle of the riser, i.e. Node 10, is represented by using the second order PC expansion. The computational results from MCS, SFEM and the proposed approach are

shown in Figure 9. The accuarcy of the obtained response variances from the proposed approach is slightly better than that from SFEM with the second order approximation. It should be noted that in this case, the SFEM with the second order approximation is employed to have a fair comparsion with the proposed approach. One possible reason is that the responses of some DOFs with a higher improtance are approximated with the third order PC expansion, which may improve the accuracy. When the PC coefficients are obtained with the mode superposition method, PDF and CDF of the horizontal deformation of the structure at the top and middle can be evaluated and shown in Figures 10 and 11. The response statistics at the top of the riser obtained from the proposed approach and SFEM with the third order PC expansion match well with those from MCS. The predicted response statistics at the middle of the riser are not as good as those at the top of the riser. This is because the truncation error associated with a lower order approximation with the second order PC expansion.

The computational time of SFEM, MCS, and the proposed multiscale method are shown in Table 1, respectively. The matirx size of the dynamic system are 40, 5460, 3640 and 18200 respectively for MCS, the proposed multiscale analysis approach, SFEM with the second order PC expansion and SFEM with the third order PC expansion, respectively. The required computation of time for each case is 12h, 2481s, 171s and 4131s, respectively. These results show the proposed approach takes less computational time than MCS and SFEM with third order PC expansion, while has a good accuracy in pedicting the response statistics.

4.2 Hollow cylinder model

A three-dimensional riser model is selected in this study to investigate the accuracy and performance of the proposed multi-scale stochastic analysis method. The segment of the riser has a length of 4 m with an outer radius of 0.1 m. The thickness of the riser is 5 mm. The mean values of the mass density and Young's modulus are 7850 kg/m^3 and 200 GPa, respectively. The numerical model of the riser is simulated with shell elements in MATLAB. Each element has 4 nodes and 24 DOFs. The mesh size is 0.5 m in the longitudinal direction, while the cross-section is discreted into 16 elements. The finite element model of the riser has totally 128 elements and 864 DOFs, as shown in Figure 12.

The spatial correlation is described by a three dimensional exponential covariance kernel as

$$C_{cov}\left((x_1,y_1,z_1),(x_2,y_2,z_2)\right)=\sigma^2 e^{-\left((x_1-x_2)^2/l_x^2+(y_1-y_2)^2/l_y^2+(z_1-z_2)^2/l_z^2\right)} \tag{52}$$

with the correlation lengths $l_x=l_y=0.05$m and $l_z=1$m. Uncertainties in the Young's modulus is considered to understand the stochastic dynamic behavior of the structure. 30% uncertainty level is considered in the Young's modulus. The lognormal random field is respresented by the first four eigenvalues and eigenvectors of KL expansion and the third order PC expansion.

The riser has a fixed end at the bottom. The sea wave loading is applied on the structure with non-uniform distribution in the y-direction. The loading is full applied from $z=4$m to 3m and linearly decreases to zero from 3m to the sea bottom. The parameters in the sea wave loading are $F=100000$ (fetch length), $v_{10}=10$m/s (mean wind velocity at 10 m above the sea surface), $d_p=0.2$m (outer diameter of the structure). The other parameters are the same as those described in Section 4.1. The uncertainties in damping is also considered in this study. The Rayleigh damping is used with the coefficients of $\alpha=3.5969$ and $\beta=5.31\times10^{-5}$.

MCS and SFEM are performed to obtain the reference values to verify the accuracy of the proposed multiscale analysis method. The results from SFEM with different orders of PC expansions are shown in Figure 13 with those results from MCS. The results from SFEM with third order PC expansions matches well with those from MCS. The results from SFEM with first/second order PC are slightly difference with those from MCS. A higher order PC expansion leads to a better result. Table 2 shows the computational time of MCS and SFEM. It takes more than 160 hours to obtain the response statistics with 50000 runs for MCS because of the complexity of the used model. It takes a less computational time for a lower order PC expansion in SFEM as shown in Table 2, however, the accuracy in the response statistics are also reduced.

The proposed approach balances the required computational time due to a higher order PC expansion, and maintains the accuracy by defining the master DOFs with a high importance and interest. The displacements along the y-direction are represented with third order PC expansion, while the displacements along the z-direction are represented with first order PC expansion. Since the responses along the y-direction are of more importance than the vertical DOFs. The deformation along the x-direction is very small, because the loads are applied in the y-z plane. These DOFs along the x-direction and all the rotational DOFs are not of interest and important, and therefore the corresponding PC coefficients of these DOFs are selected as the slave ones. The third order PC expansion is performed to obtain system matrices (M_s and K_s) and then IOR method is used to eliminate the unwanted slave DOFs to obtain M_r and K_r. The stochastic dynamic analysis is then conducted and the response results are shown in Figures 14 and 15, comparing with the results from SFEM and MCS. For the responses along the y direction, the random output is represented with third order PC expansion. The results of

response statistics match well with those results from MCS and SFEM with the third order PC expansion, as shown in Figure 14. The results from the low order PC expansion is shown in Figure 15. The mean values of responses from MCS, SFEM with the first order, and the proposed approach are almost the same, while the variance is slightly different from those results from MCS but better than SFEM with the first order PC expansion only. Figure 16 compares the obtained PDF of the displacement response with different methods. Those DOFs with higher order expansions have a good accuracy, matching well with the results from SFEM and MCS. For those DOFs with lower order expansions, there is some minor difference due to the errors associated with the low order PC expansions to represent the responses. Table 2 shows the matrix size and the computational time. The computational time required for MCS is about 160 hours, however, the proposed multi-scale analysis method takes about 0.5 hour. The results show that the computational efficiency is significantly improved with the proposed method and the accuracy is the same as those from MCS.

5 Conclusions

Using Gaussian random fields to simulate the uncertain system parameters has been studied. However, this assumption is not necessarily true and suitable to model all the material properties. In this paper, the uncertainties in the mass density and Young's modulus are assumed having lognormal distributions, which is different from previous works but more realistically modelled. The lognormal random fileds are represented by a combination of KL and PC expansions. A multi-scale stochastic dyanmic analysis method is developed to evaluate the response statistics of marine risers, considering the lognormal uncertainties in the material parameters. The random outputs, such as stochastic

displacement, are approximated with different orders of PC expansions. High accuracy of uncertainty analysis results can be obtained for those responses approximated with a high order PC expansion. Responses at those DOFs with less and least importances are represented with low order PC expansions to reduce the matix size of the stochastic dynamic system and the computational efforts. Therefore three categories of DOFs are defined, namely, (a) important ones with high order PC expansions; (b) less important ones with low order PC expansions, and (c) the least important ones to be eliminated. Model reduction technique, i.e. IOR method, is used to eliminate the slave PC coefficients, and the multi-scale stochastic dynamic response analysis is performed. The response statistics are obtained from the PC coefficients directly, and compared with those from MCS and SFEM. Numerical studies on marine risers with lognormal uncertainties in material properties are conducted. The results from the proposed method match well with those from MCS, with significantly less computational time required. The computational demand is significantly reduced with the model reduction technique, however, the accuracy of the stochastic response analysis results keeps the same.

References

Alibrandi, U., Koh, C., 2017. Stochastic dynamic analysis of floating production systems using the first order reliability method and the secant hyperplane method. Ocean Engineering 137, 68-77.

Barbato, M., Gu, Q., Conte, J., 2010. Probabilistic push-over analysis of structural and soil-structure systems. Journal of structural engineering 136 (11), 1330-1341.

Barbato, M., Zona, A., Conte, J.P., 2013. Probabilistic nonlinear response analysis of steel-concrete composite beams. Journal of structural engineering 140 (1), 04013034.

Borino, G., Muscolino, G., 1986. Mode‐superposition methods in dynamic analysis of classically and non‐classically damped linear systems. Earthquake Engineering & Structural Dynamics 14 (5), 705-717.

Cabrera-Miranda, J.M., Paik, J.K., 2017. On the probabilistic distribution of loads on a marine riser. Ocean Engineering 134, 105-118.

Cabrera-Miranda, J.M., Paik, J.K., 2019. Two-phase flow induced vibrations in a marine riser conveying a fluid with rectangular pulse train mass. Ocean Engineering 174, 71-83.

Chen, W., Li, M., Zheng, Z., Guo, S., Gan, K., 2015. Impacts of top-end vessel sway on vortex-induced vibration of the submarine riser for a floating platform in deep water. Ocean Engineering 99, 1-8.

Dolinski, K., 1982. First-order second-moment approximation in reliability of structural systems: critical review and alternative approach. Structural Safety 1 (3), 211-231.

Feng, X., Wu, W., Meng, D., Ansari, F., Zhou, J., 2017. Distributed monitoring method for upheaval buckling in subsea pipelines with Brillouin optical time-domain analysis sensors. Advances in Structural Engineering 20 (2), 180-190.

Friswell, M., Garvey, S., Penny, J., 1995. Model reduction using dynamic and iterated IRS techniques. Journal of Sound and Vibration 186 (2), 311-323.

Ghanem, R.G., Spanos, P.D., 2003. Stochastic finite elements: a spectral approach. Courier Corporation.

Gupta, A., Arun, C., 2018. Stochastic meshfree method for elastic buckling analysis of columns. Computers & Structures 194, 32-47.

Guyan, R.J., 1965. Reduction of stiffness and mass matrices. Aiaa Journal 3 (2), 380-380.

Haldar, A., Mahadevan, S., 2000. Reliability assessment using stochastic finite element analysis. John Wiley & Sons.

Haukaas, T., Der Kiureghian, A., 2004. Finite element reliability and sensitivity methods for performance-based earthquake engineering. Pacific Earthquake Engineering Research Center, College of Engineering, University of California, Berkeley.

He, J.W., Low, Y.M., 2013. Predicting the Probability of Riser Collision Under Stochastic Excitation and Multiple Uncertainties. Journal of Offshore Mechanics and Arctic Engineering 135 (3), 031602.

Hong, K.-S., Shah, U.H., 2018. Vortex-induced vibrations and control of marine risers: A review. Ocean Engineering 152, 300-315.

Huang, S., Quek, S., Phoon, K., 2001. Convergence study of the truncated Karhunen–Loeve expansion for simulation of stochastic processes. International Journal for Numerical Methods in Engineering 52 (9), 1029-1043.

Kiureghian, A.D., Fujimura, K., 2009. Nonlinear stochastic dynamic analysis for performance‐based earthquake engineering. Earthquake Engineering & Structural Dynamics 38 (5), 719-738.

Koh, K., Yassin, A.M., Latheef, M., 2018. On the buoyancy load formulation for geometrically nonlinear analysis of flexible marine risers. Ocean Engineering 157, 313-324.

Li, C.-C., Der Kiureghian, A., 1993. Optimal discretization of random fields. Journal of Engineering Mechanics 119 (6), 1136-1154.

Li, J., Law, S., 2012. Damage identification of a target substructure with moving load excitation. Mechanical Systems and Signal Processing 30, 78-90.

Li, X., Guo, X., Guo, H., 2018. Vector form intrinsic finite element method for nonlinear analysis of three-dimensional marine risers. Ocean Engineering 161, 257-267.

Ni, P., Li, J., Hao, H., Xia, Y., 2018. Stochastic dynamic analysis of marine risers considering Gaussian system uncertainties. Journal of Sound and Vibration 416, 224-243.

Patel, M., Seyed, F., 1995. Review of flexible riser modelling and analysis techniques. Engineering Structures 17 (4), 293-304.

Saydam, D., Frangopol, D.M., 2013. Applicability of simple expressions for bridge system reliability assessment. Computers & Structures 114, 59-71.

Stefanou, G., 2009. The stochastic finite element method: past, present and future. Computer Methods in Applied Mechanics and Engineering 198 (9-12), 1031-1051.

Sudret, B., Der Kiureghian, A., 2000. Stochastic finite element methods and reliability: a state-of-the-art report. Department of Civil and Environmental Engineering, University of California Berkeley, CA.

Teixeira, D.C., Morooka, C.K., 2017. A time domain procedure to predict vortex-induced vibration response of marine risers. Ocean Engineering 142, 419-432.

Torres, L., Verde, C., Vázquez-Hernández, O., 2015. Parameter identification of marine risers using Kalman-like observers. Ocean Engineering 93, 84-97.

Tsukada, R.I., Morooka, C.K., 2016. A numerical procedure to calculate the VIV response of a catenary riser. Ocean Engineering 122, 145-161.

Veritas, N., 2000. Environmental conditions and environmental loads. Det Norske Veritas.

Walden, H., Richter, K., Sell, W., Olbers, D., Meerburg, A., Bouws, E., Carlson, H., Barnett, T., Hasselmann, K., Cartwright, D., 1973. Measurements of wind-wave growth and swell decay during the Joint North Sea Wave Project (JONSWAP). Ergänzungsheft 8-12.

Wan, H.-P., Todd, M.D., Ren, W.-X., 2017. Statistical Framework for Sensitivity Analysis of Structural Dynamic Characteristics. Journal of Engineering Mechanics 143 (9), 04017093.

Weng, S., Tian, W., Zhu, H., Xia, Y., Gao, F., Zhang, Y., Li, J., 2017. Dynamic condensation approach to calculation of structural responses and response sensitivities. Mechanical Systems and Signal Processing 88, 302-317.

Wiener, N., 1938. The Homogeneous Chaos. American Journal of Mathematics 60 (4), 897-936.

Wu, Z., Liu, J., Liu, Z., Lu, Z., 2016. Parametrically excited vibrations of marine riser under random wave forces and earthquake. Advances in Structural Engineering 19 (3), 449-462.

Xia, Y., Lin, R.M., 2004a. Improvement on the iterated IRS method for structural eigensolutions. Journal of Sound and Vibration 270 (4-5), 713-727.

Xia, Y., Lin, R.M., 2004b. A new iterative order reduction (IOR) method for eigensolutions of large structures. International Journal for Numerical Methods in Engineering 59 (1), 153-172.

Xiu, D., Karniadakis, G.E., 2002. The Wiener--Askey polynomial chaos for stochastic differential equations. SIAM journal on scientific computing 24 (2), 619-644.

Xiu, D., Karniadakis, G.E., 2003. Modeling uncertainty in flow simulations via generalized polynomial chaos. Journal of Computational Physics 187 (1), 137-167.

Yamazaki, F., Member, A., Shinozuka, M., Dasgupta, G., 1988. Neumann expansion for stochastic finite element analysis. Journal of Engineering Mechanics 114 (8), 1335-1354.

Yang, H., Wang, A., 2013. Dynamic stability analysis of pipeline based on reliability using surrogate model. Journal of Marine Engineering & Technology 12 (2), 75-84.

Zuo, H., Bi, K., Hao, H., 2017. Using multiple tuned mass dampers to control offshore wind turbine vibrations under multiple hazards. Engineering Structures 141, 303-315.

Table 1 Matrix size and computational time for the riser simulated as a beam model

Method	The proposed approach	SFEM (The second order PC expansion)	SFEM (The third order PC expansion)	MCS
Matrix size	5460	3640	18200	40
Computational time	2481s	171s	4131s	12h

Table 2 Matrix size and computational time for the riser simulated as a cylinder model

Method	The proposed approach	SFEM (2nd)	SFEM (3rd)	MCS
Matrix size	5120	3840	26880	768
Computational time	2137s	203s	4762s	160h
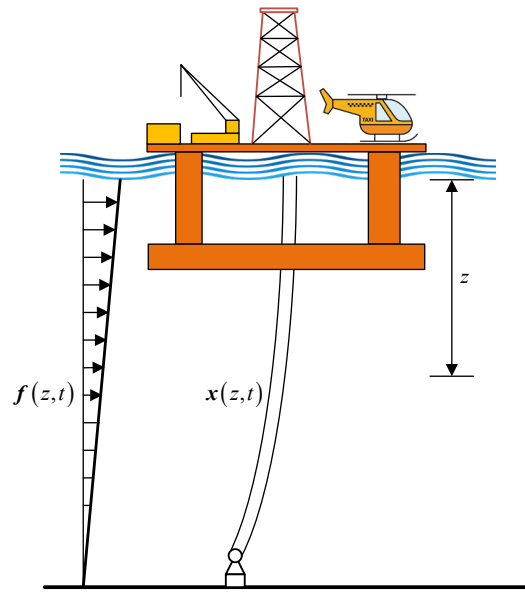
Figure 1 Schematic of a marine riser
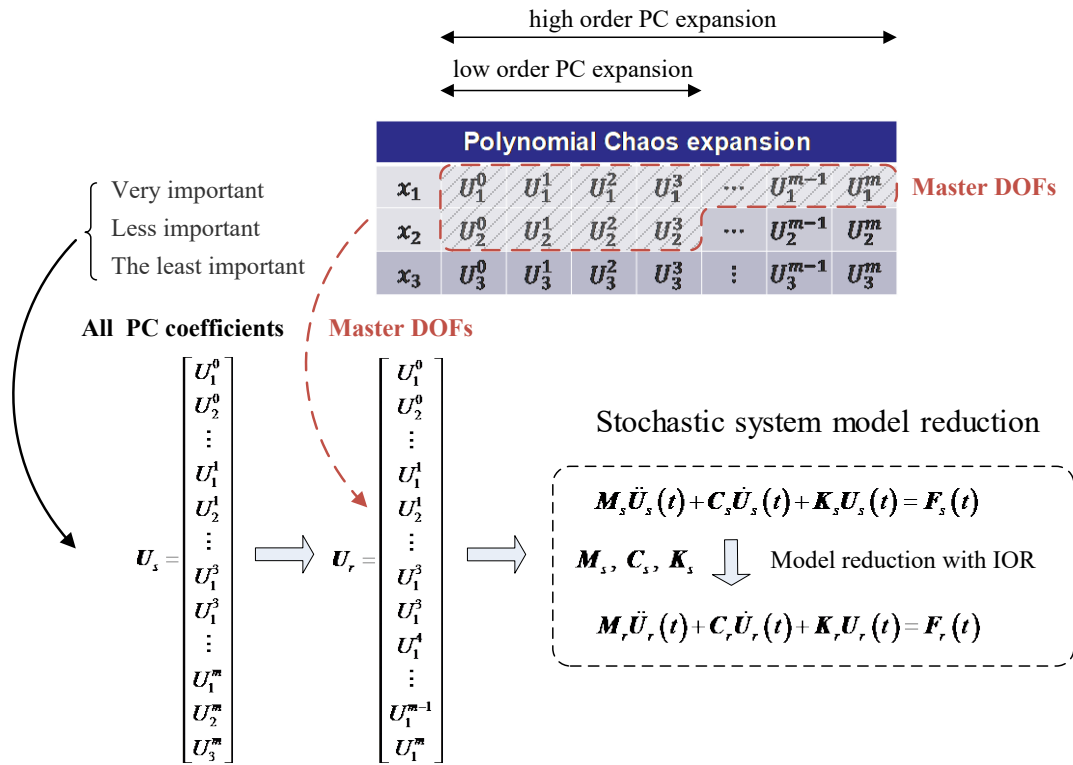
Figure 2 Categories of the DOFs in the model reduction
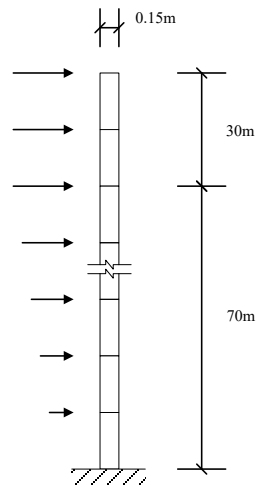
Figure 3 Numerical model of a riser
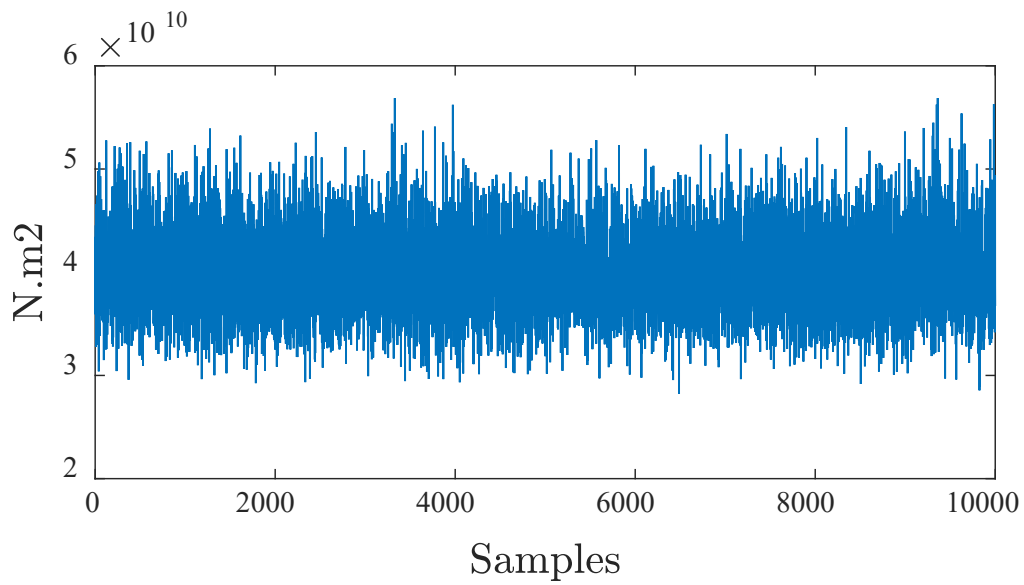
(a) represented random input with KL and PC expansions
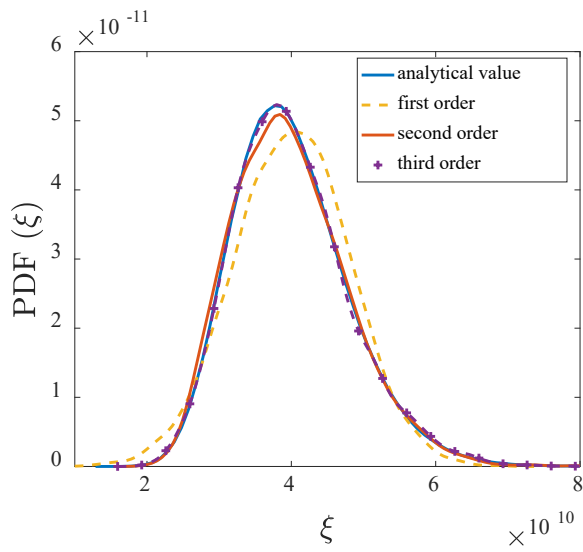
(b) PDF of the represented random input
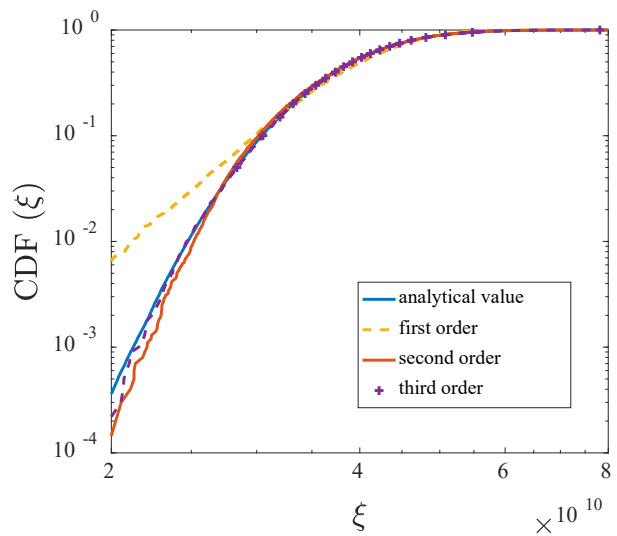
(c) CDF of the represented random input

Figure 4 Representation of random fields
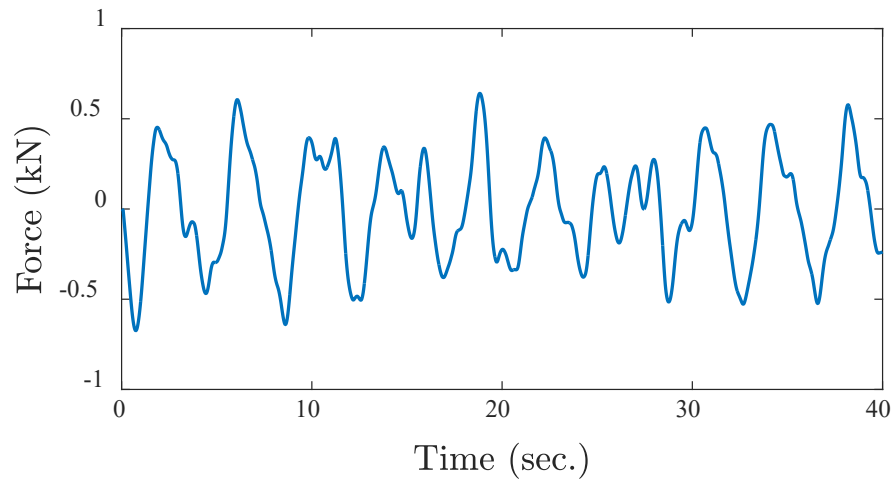
Figure 5 Sea wave loading
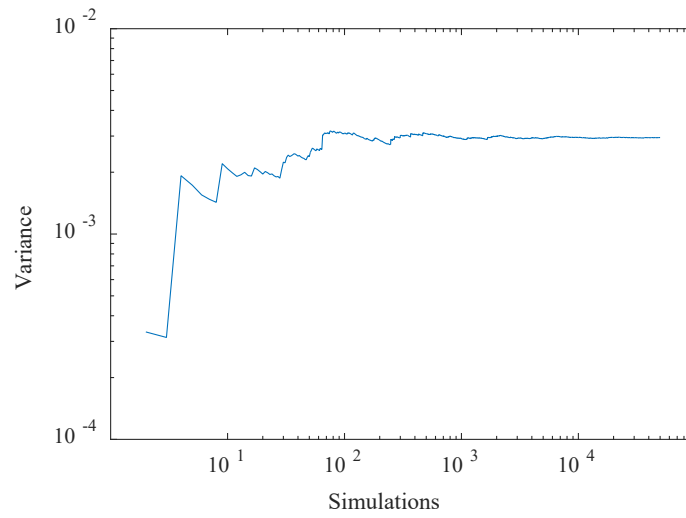
(a) Convergence of response variance at the top of the riser at
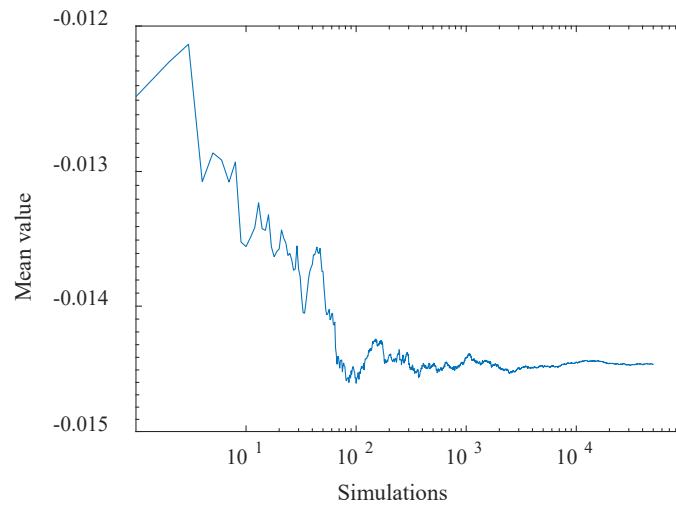
t=30s

(b) Convergence of response mean value at the top of the riser

at t=30s

Figure 6 Convergence analysis of MCS with different numbers of simulations
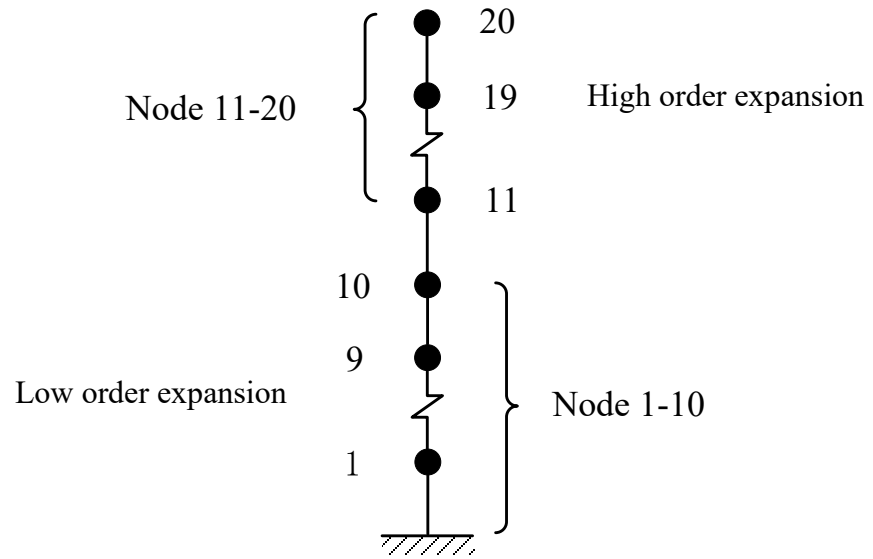
Figure 7 Selection of orders in PC expansions
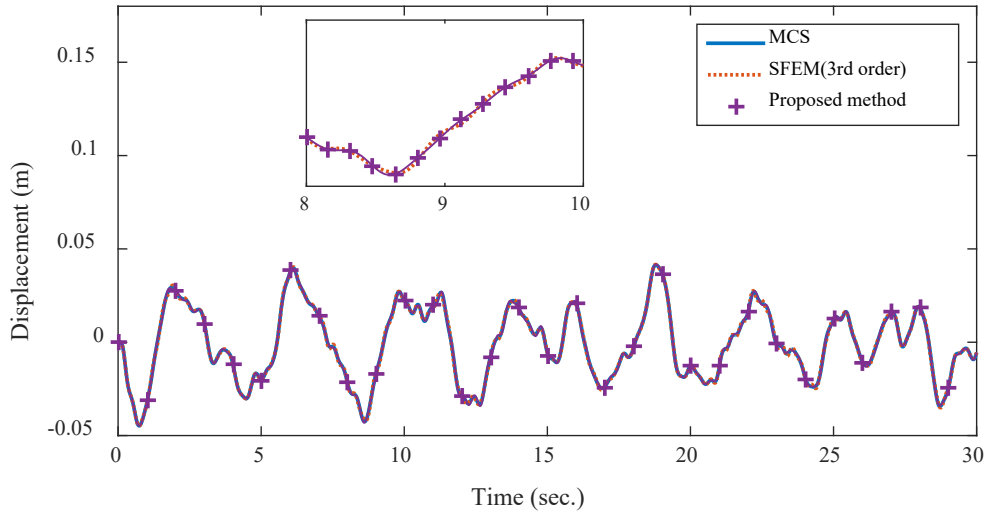
(a) Mean value
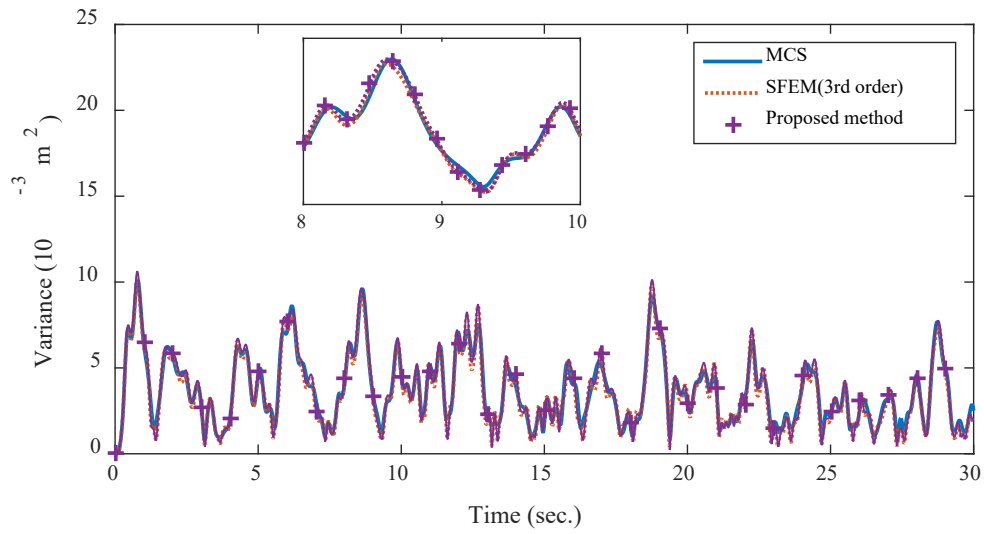
(b) Variance

Figure 8 Response statistics of the horizontal displacement at the top end of the riser
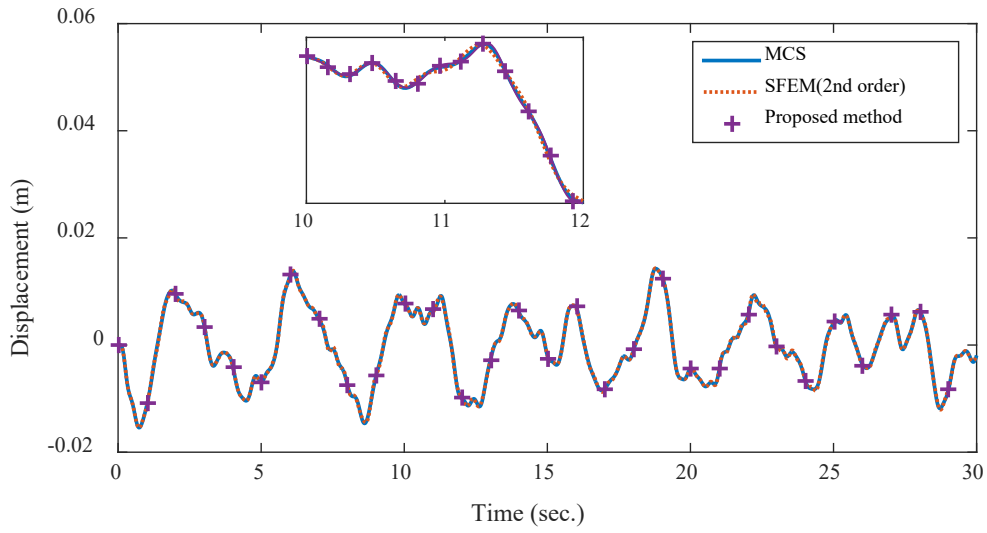
(a) Mean value
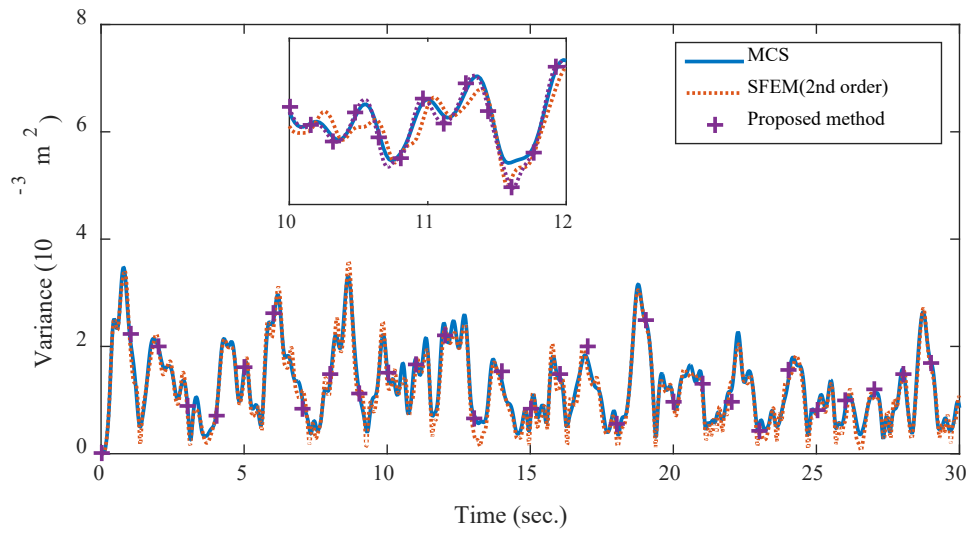
(b) Variance

Figure 9 Response statistics of the horizontal displacement at the middle of the riser
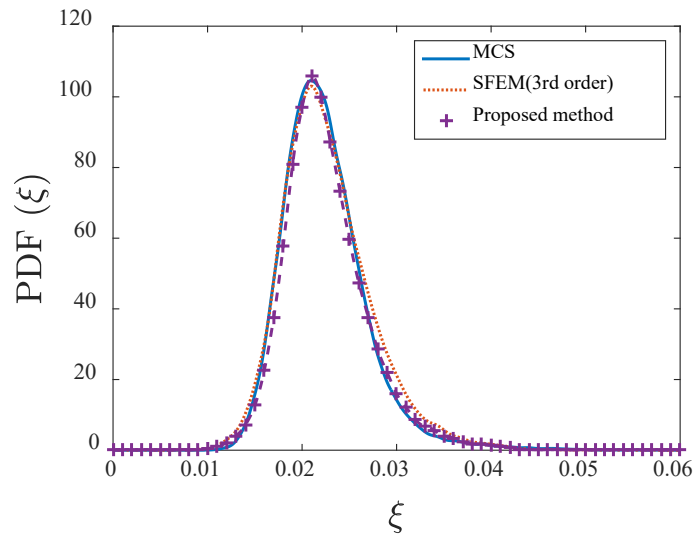
(a) PDF
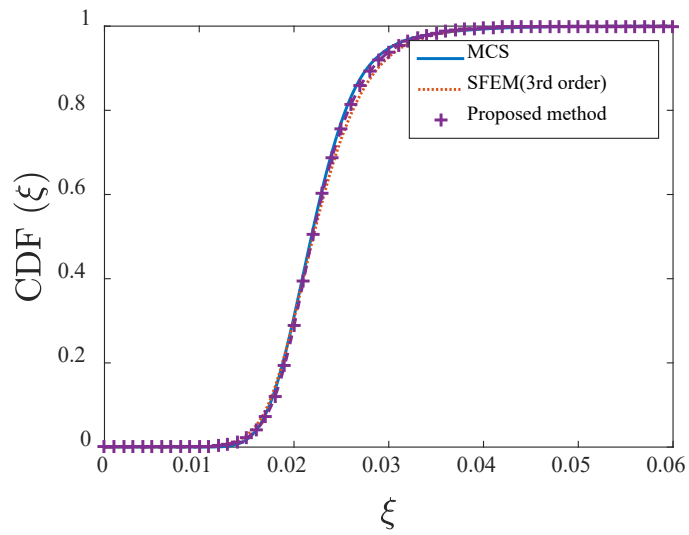
(b) CDF

Figure 10 Probability distribution of the response at the top end of the riser with MCS, SFEM

and the proposed approach at t=30s
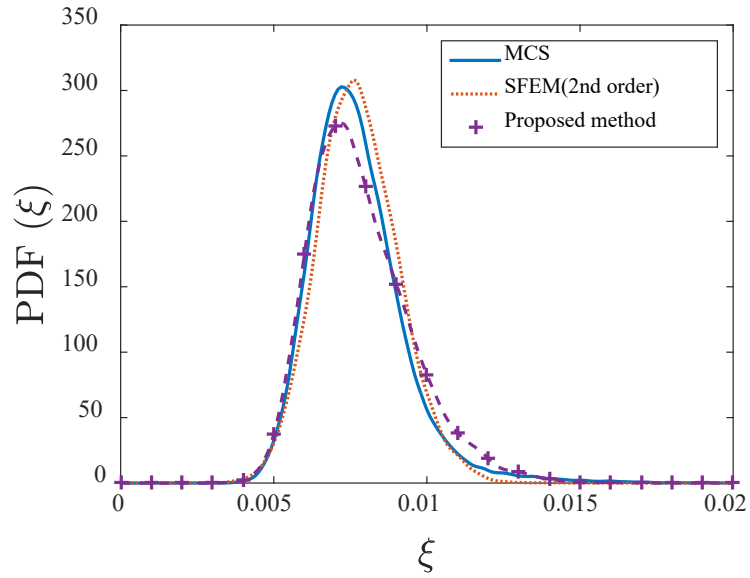
(a) PDF
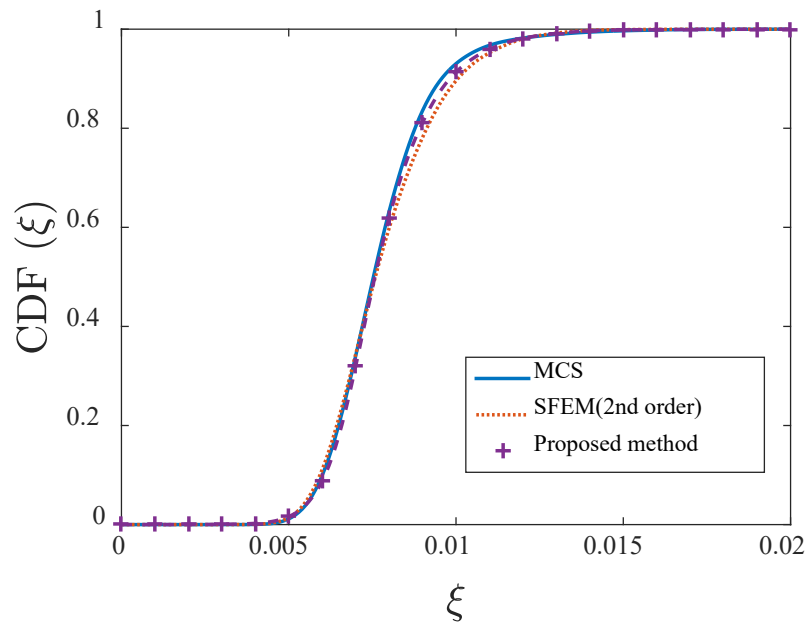
(b) CDF

Figure 11 Probability distribution of the response at the middle of the riser with MCS, SFEM

and the proposed approach at t=30s

Critical point

wave loading

z

x

y
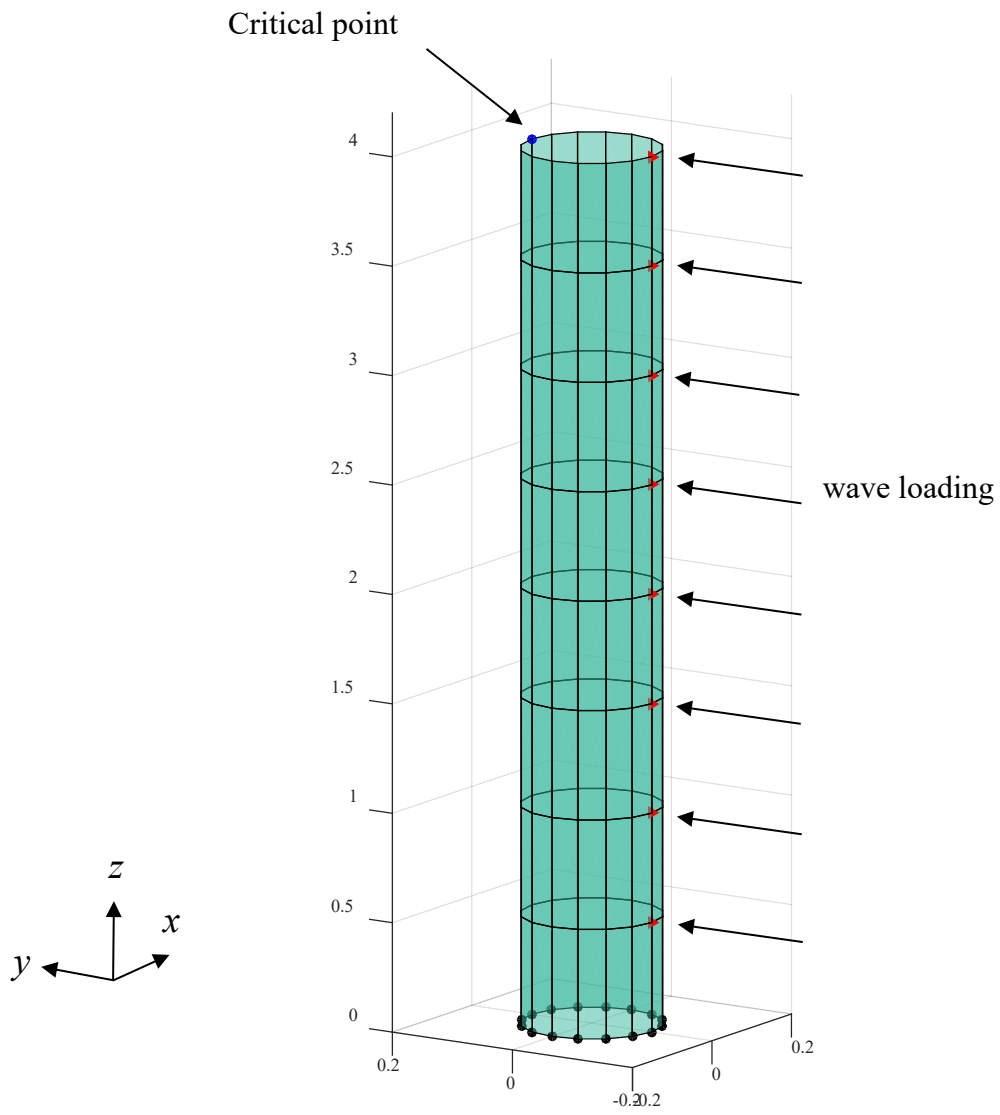
Figure 12 Hollow cylinder model
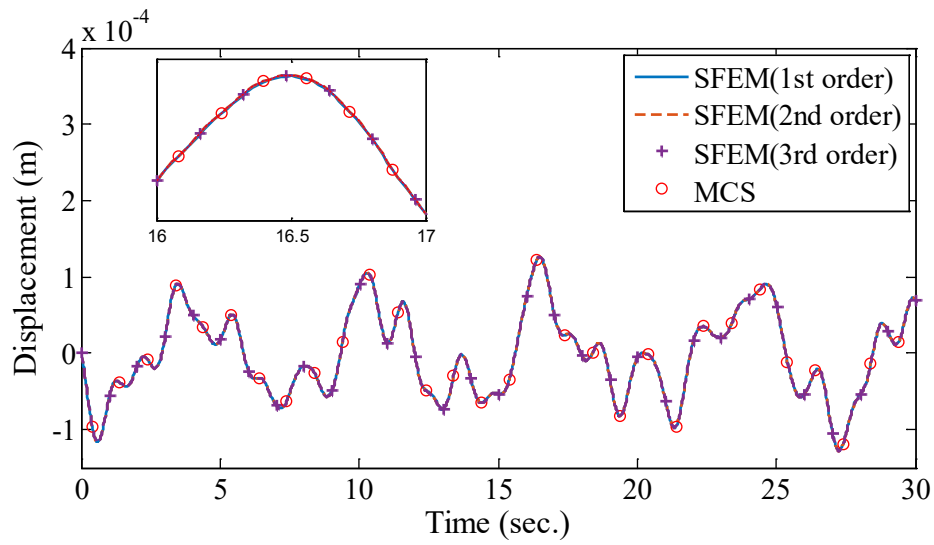
(a) Mean value
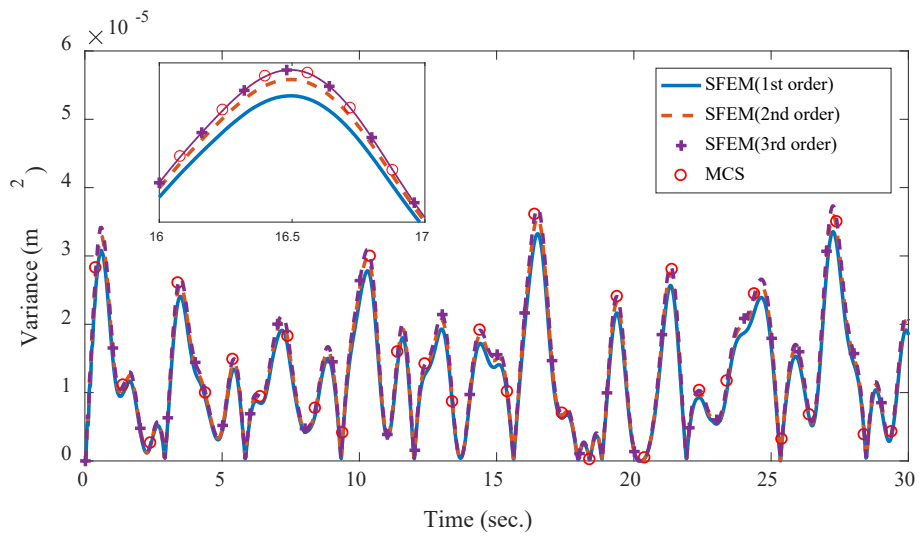
(b) Variance

Figure 13 Response statistics of the displacement at the critical point along y-direction from SFEM
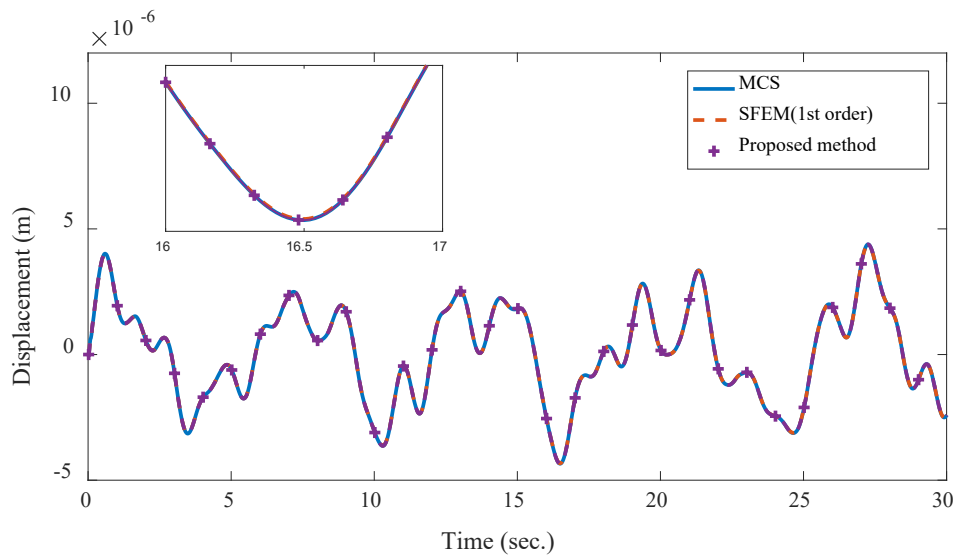
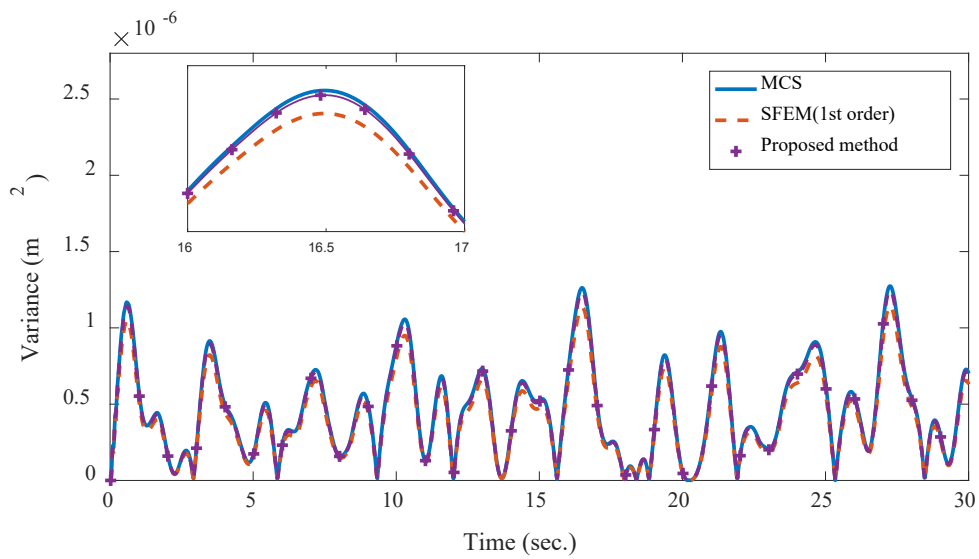with different orders of PC expansions and MCS
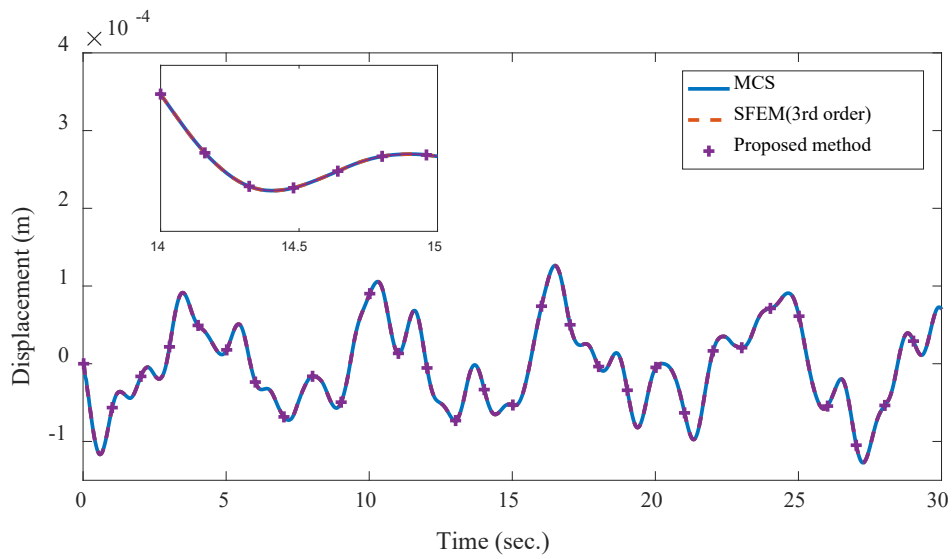
(a) Mean value
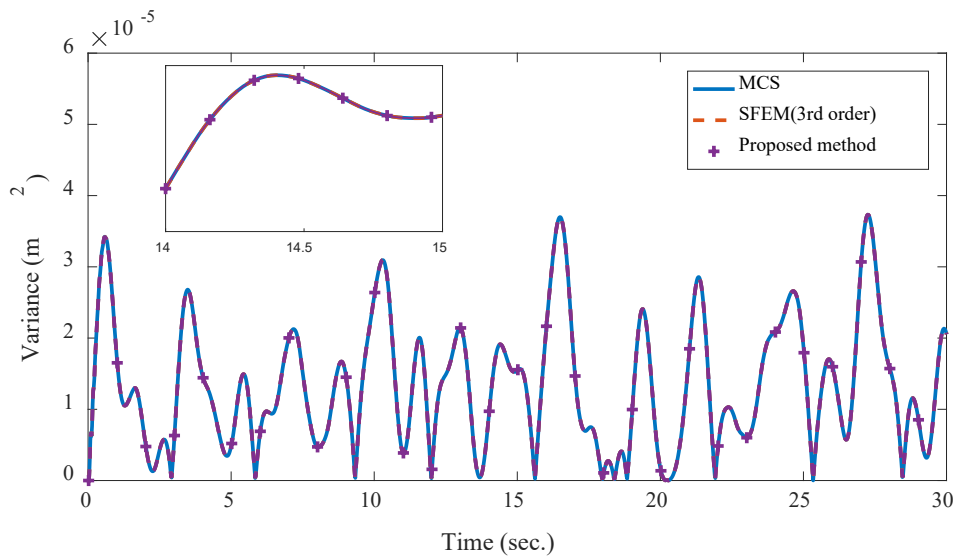
(b) Variance

Figure 14 Response statistics of the displacement at the critical point along *y*-direction from different
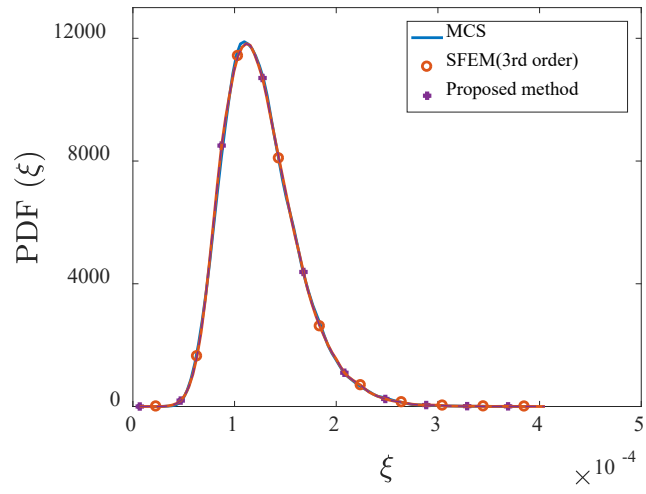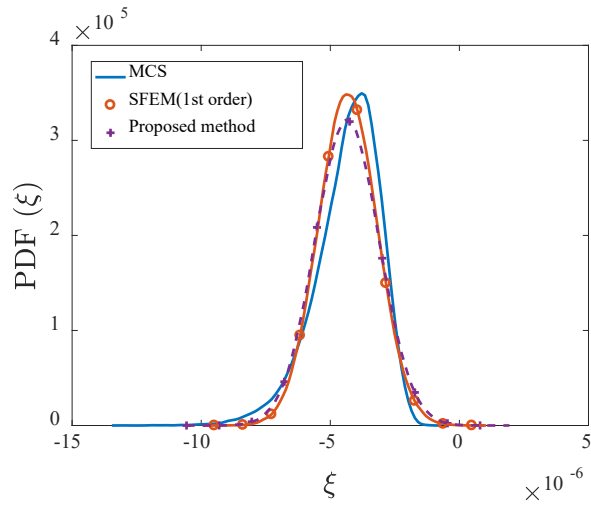
methods

(a) Mean value

(b) Variance

Figure 15 Response statistics of the displacement at the critical point along *z*-direction from different

methods

(a) PDF of response at the critical point along *y*-direction

(t=16.5s)

(b) PDF of the response at the critical point along *z*-

direction (t=16.5s)

Figure 16 PDF of the responses at the critical point from the different methods